AIP | Review of Scientific Instruments

A method for coincidence timing resolution enhancement

E. E. Ermis, C. Celiktas, and E. Pilicer

Citation: Review of Scientific Instruments **87**, 053504 (2016); doi: 10.1063/1.4948925
View online: http://dx.doi.org/10.1063/1.4948925
View Table of Contents: http://scitation.aip.org/content/aip/journal/rsi/87/5?ver=pdfcov
Published by the AIP Publishing

Articles you may be interested in

Performance characterization of high quantum efficiency metal package photomultiplier tubes for time-of-flight and high-resolution PET applications
Med. Phys. **42**, 510 (2015); 10.1118/1.4903897

Detection of special nuclear materials with the associate particle technique
AIP Conf. Proc. **1525**, 220 (2013); 10.1063/1.4802323

Time-of-flight system with a movable ion detector for absolute measurement of cyclotron beam energy
Rev. Sci. Instrum. **76**, 113106 (2005); 10.1063/1.2135285

emiT: An apparatus to test time reversal invariance in polarized neutron decay
Rev. Sci. Instrum. **75**, 5343 (2004); 10.1063/1.1821628

A highly efficient neutron time-of-flight detector for inertial confinement fusion experiments
Rev. Sci. Instrum. **70**, 1221 (1999); 10.1063/1.1149430



Reuse of AIP Publishing content is subject to the terms at: https://publishing.aip.org/authors/rights-and-permissions. Download to IP: 155.223.84.191 On: Mon, 17 Oct 2016 10:49:28

A method for coincidence timing resolution enhancement

E. E. Ermis,[1,a)] C. Celiktas,[1] and E. Pilicer[2]
[1]*Faculty of Science, Physics Department, Ege University, 35100 Bornova, Izmir, Turkey*
[2]*Faculty of Arts and Science, Physics Department, Uludag University, Gorukle, Bursa, Turkey*

(Received 3 February 2016; accepted 27 April 2016; published online 12 May 2016)

A method including the coincidence time resolution improvement for a TOF/positron emission tomography system was suggested. The spectrometer for this aim was composed of two NaI(Tl) and two plastic scintillation detectors. Experimental results were supported by FLUKA Monte Carlo simulation program by constructing the detector setup in software medium. Present experimental results verified our previous results and conclusions obtained from the suggested method. It was concluded that better resolutions would help the improvement not only on the TOF gain but also on the spatial resolution, leading to better images and helping the Physician in his/her diagnosis and treatment. *Published by AIP Publishing.* [http://dx.doi.org/10.1063/1.4948925]

I. INTRODUCTION

In a PET (Positron Emission Tomography) system, two gamma photons are detected simultaneously by two detectors (start and stop detectors) in coincidence within a given time interval. Its measurement sensitivity, i.e., image quality depends on the time resolution of the used coincidence spectrometer.

Some physical terms are used to express the properties of an imaging system. Spatial resolution is one of them. It is defined as the minimum distance between two points in an object which means that it can be observed as two distinct points in an image.[1] In a timing system, the FWHM value, width of a peak at half its full height, of the time spectrum determines the time resolution. Lower time resolution value is better timing, i.e., better time-detection. And also, the overall timing uncertainty can be identified by using this FWHM value of the time distribution in a spectrometer.[2] Localization uncertainty of the coincidence system (Δx) can be defined as spatial resolution. It is calculated from $\Delta x = c\Delta t/2$,[3–13] where c and Δt are the speed of light and time resolution of the system, respectively. In this equation, c is used because the photons travel at the speed of light (Fig. 1).

Multiplicative reduction factor (f) is another parameter of a coincidence measurement system. This factor (corresponding to the reduction in noise variance) is found by dividing D which is called as the size of the emission source or radial dimension of the object to be imaged to Δx[4,6,14,15] ($f = D/\Delta x$). The SNR (signal-to-noise ratio) gain due to TOF or TOF gain (G) of a spectrometer can be expressed as the square root of f ($\sqrt{f}$).[4,8,10,11,15,16] In order to achieve better detection performance, higher G values should be obtained.

In a timing measurement, there are two important parameters; peaking and shaping times. The time required for a pulse to reach its amplitude is called as peaking time.[2] The shaping time is the corresponding time to 61% of a timing peak value. The relationship between these two quantities is that the peaking time is approximately 3-5 times greater than the shaping time (Fig. 2).[17]

FLUKA is a Monte Carlo (MC) simulation program. It is a general purpose tool for calculations of particle transport and interactions with matter, covering and extended range of applications spanning from proton and electron accelerator shielding to target design, dosimetry, detector design, etc. Interaction and propagation in matter of any particle can also be simulated by means of FLUKA.[18,19]

In a medical imaging system, the time resolution is an important parameter because image quality depends on it. Therefore, time resolution values should be determined very precisely. In the present study, the same experimental method in our previous work[20] is proposed to enhance the time resolution of a coincidence system composed of start-stop detectors. In the first part of the study, coincidence measurements were separately carried out using spectrometers consisting of NaI(Tl) and BC412 type plastic scintillation detectors by changing the distances between the source and the start detectors. The coincidence time resolution (or resolving time) and delay time for each distance were determined by using the constant fraction timing method. In the second part of the study, time resolution was calculated by applying additional delay to the input of the timing signal to enhance the time resolution and TOF gain values of the spectrometers. The experimental results were compared with the results from the FLUKA MC program. This study has supported our previous method to enhance the TOF/PET time resolution.[20]

II. MATERIALS AND METHODS

We have followed the experimental method suggested in our previous work[20] to improve the coincidence time resolution of a TOF/PET system. The difference of the presented study from the previous one is that we used a positron source and different type of plastic scintillators (BC412) here to show the validity of our suggested method in enhancing the time resolution of a coincidence timing measurement.

A solid point ^{22}Na positron source with the activity of ~5 μCi was used in the experiments for two annihilation quanta.

a)Electronic mail: elermis@hotmail.com

Reuse of AIP Publishing content is subject to the terms at: https://publishing.aip.org/authors/rights-and-permissions. Download to IP: 155.223.84.191 On: Mon, 17 Oct 2016 10:49:28

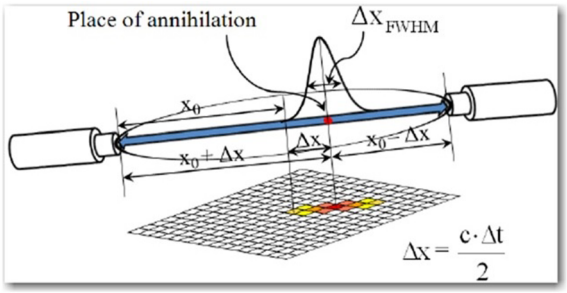


FIG. 1. Illustration of TOF/PET principle.

Two Rexon NaI(Tl) with the decay time of 250 ns[21] and two Saint Gobain BC412 type plastic with the decay time of 3.3 ns[22] scintillation detectors were used in the experiments to obtain start-stop coincidence measurements. Both detector types had cylindrical shapes. In Fig. 3, the dimensions of the

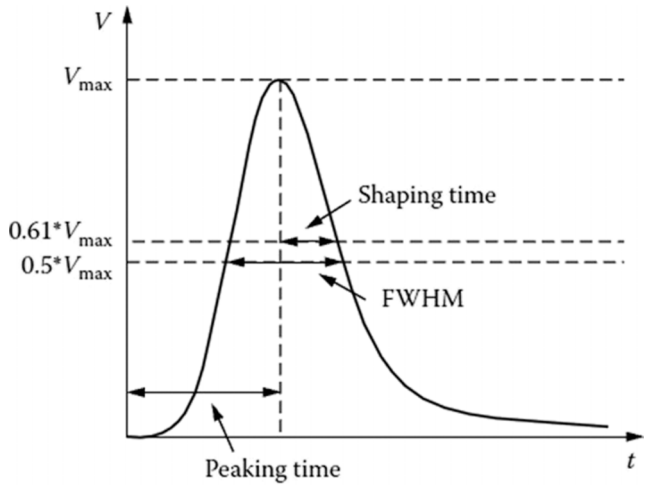


FIG. 2. Definitions of shaping and peaking times in a time spectrum.

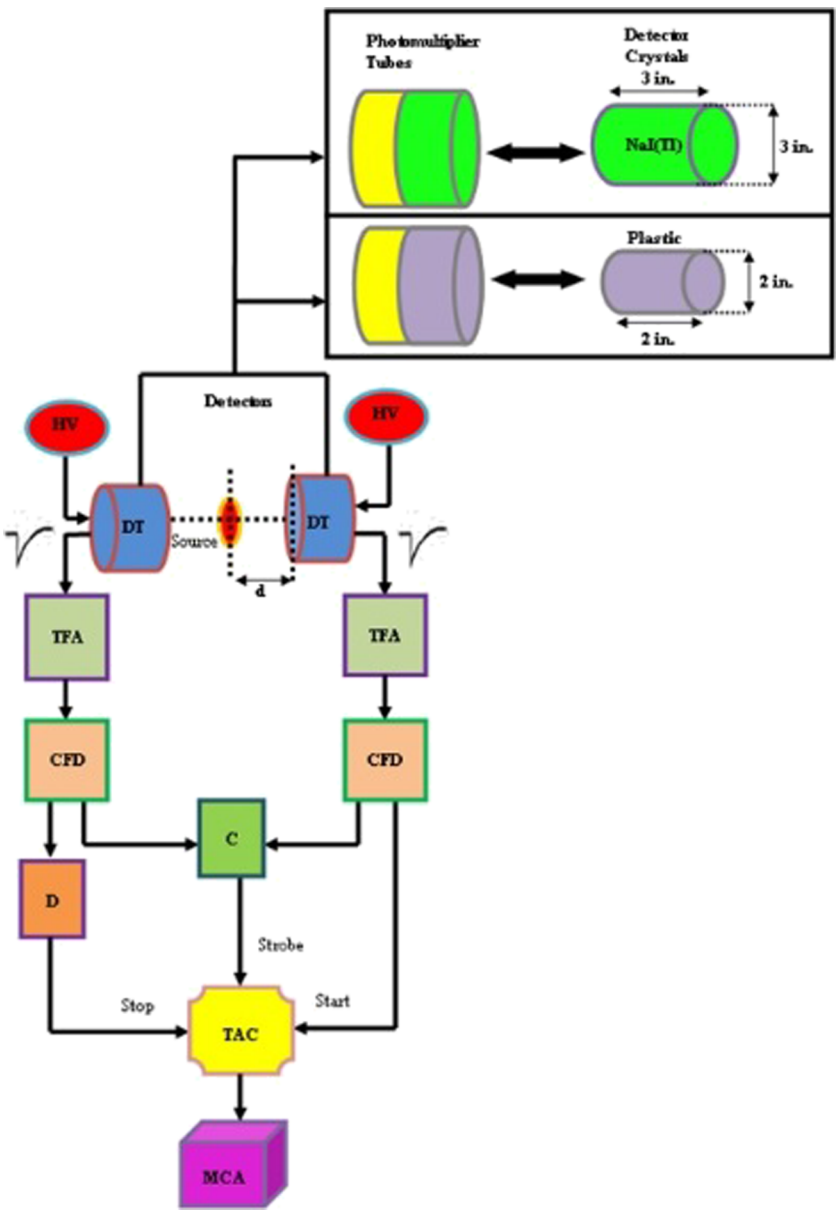


FIG. 3. Block diagram of the spectrometer.

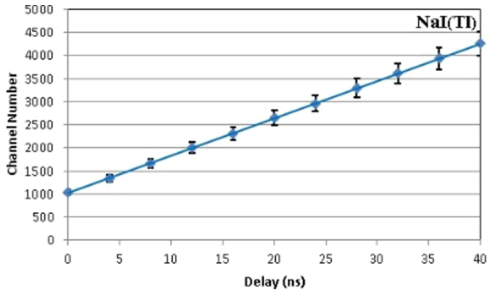
Reuse of AIP Publishing content is subject to the terms at: https://publishing.aip.org/authors/rights-and-permissions. Download to IP: 155.223.84.191 On: Mon, 17 Oct 2016 10:49:28

used detector crystals are given. The detectors were first placed 2 cm apart. The radioactive source was placed in their central position between them. This position was set as reference point. While the stop detector was fixed, the start detector was placed in the distances of d = 2,4,6,8 cm from the source, respectively. The data acquisition time for both detector types was chosen as 300 s. Since ambient light and high temperature led to detector noise, the measurements were taken at the constant temperature of 22 °C and in a dark room.[23]

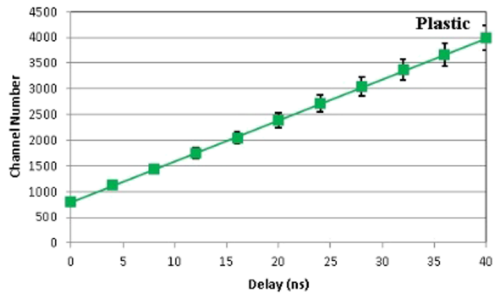
Constant fraction timing method was used in the presented study. In this timing measurement method, a walk-free timing signal is generated, giving an advantage of optimum triggering and best time resolution.[23] It is possible to find further information about the method in Refs. 2 and 23–25.

The block diagram of the used spectrometer, which was used to acquire the time spectrum of ^{22}Na, is given in Fig. 3. NaI(Tl) and plastic scintillation detectors were used in this spectrometer. In the spectrometer, detectors were mounted on the photomultiplier tubes (PMTs, Ortec 266). The anode outputs which give fast negative signal of these tubes were connected to timing filter amplifiers (TFAs, Ortec 454). The aim of TFA usage was to amplify the signal and reduce the high-frequency noise via its selectable integration time.[26] The TFA outputs were connected to constant fraction discriminators (CFDs, Ortec 463). A CFD module is used to trigger on a constant fraction of the detector signal which it is independent of the signal amplitude.[27] One of the negative outputs of the CFDs was directly sent to the "start" input of a time to amplitude converter (TAC, Ortec 566). The negative output of the other CFD was first sent to a delay unit (D, Ortec 425A) and then connected to "stop" input of the TAC. The delay unit provides a time delay between "start" and "stop" inputs of the TAC. A TAC converts the time difference between its two input signals to a voltage pulse whose height is proportional to this difference between the signals. Hence, a pulse whose height corresponds to this time value is generated.[24] Positive outputs of the CFDs were connected to a coincidence module (C, Ortec 418A) to trigger the TAC through its strobe input. Consequently, the time spectra were obtained using the logic output of the TAC. A multichannel analyzer (MCA, Ortec Trump 8K) was utilized to acquire coincidence time spectrum of the two detectors. Since fast negative signals were used in the experiments, all modules were connected with RG-58 C/U type coaxial cables.

Firstly, the MCA was calibrated to designate the time value per channel. This process was repeated for each detector type. For this, we have set the TAC range and MCA conversion gain as 100 ns and 8192 ch, respectively, after many tests for the best timing resolution. Their time calibration graphs can be observed in Fig. 4. In the time calibration process, the delay time was gradually increased from zero to 40 ns with the increments of 4 ns by using delay unit shown in Fig. 3. The peak positions of time peaks versus delay time increments were plotted for NaI(Tl) and plastic detectors (Fig. 4). The time calibration graphs for both detectors were acquired in order to determine the time per channel. This value was calculated by taking the inverse of the slope of the each graph. These values for NaI(Tl) and plastic detectors were obtained as 12.29 ± 0.08 and 12.36 ± 0.15 ps/ch, respectively. The time value per

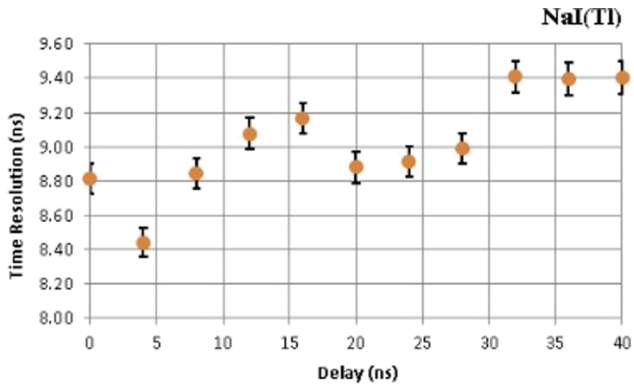


(a) Time calibration graph for the NaI(Tl) scintillation detector (fitted time calibration=12.29±0.08 ps/ch.)

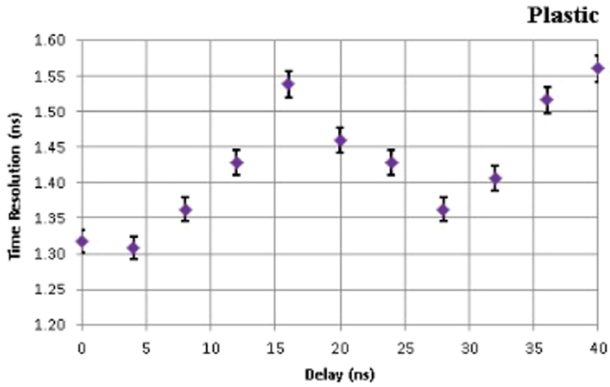


(b) Time calibration graph for the plastic scintillation detector (fitted time calibration=12.36±0.15 ps/ch.)

FIG. 4. (a) Time calibration graph for the NaI(Tl) scintillation detector. (b) Time calibration graph for the plastic scintillation detector.



(a) Optimum delay time graph for the NaI(Tl) scintillation detector.



(b) Optimum delay time graph for the plastic scintillation detector.

FIG. 5. (a) Optimum delay time graph for the NaI(Tl) scintillation detector. (b) Optimum delay time graph for the plastic scintillation detector.

Reuse of AIP Publishing content is subject to the terms at: https://publishing.aip.org/authors/rights-and-permissions. Download to IP: 155.223.84.191 On: Mon, 17 Oct 2016 10:49:28

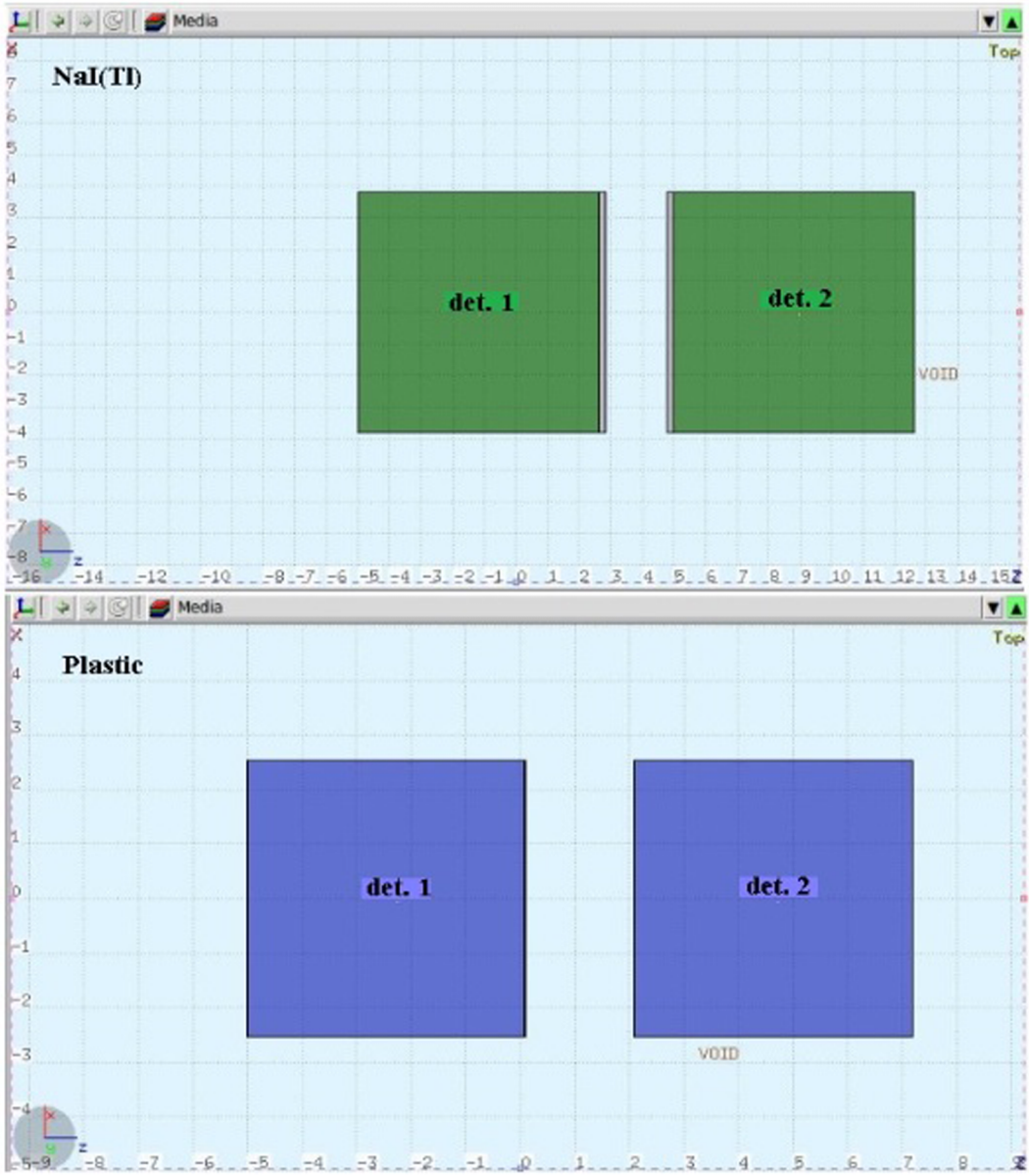


FIG. 6. Simulated detectors' positions in FLUKA.

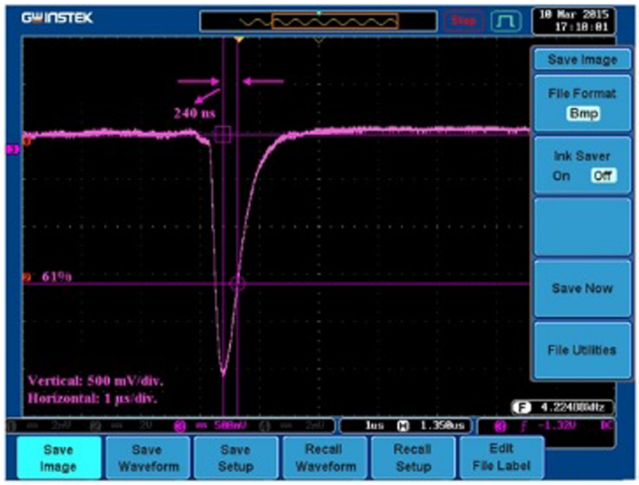
channel was also calculated using TAC range and the conversion gain of the MCA to check the values obtained from the calibration graphs. This time value per channel was calculated as 12.21 ps/ch by dividing 100 ns (TAC range) to 8192 ch (conversion gain of the MCA). The values from calibration graphs were highly close to the real one (12.21 ps/ch) for both detector types.

Optimum delay time (which is called a time differences between start-stop inputs of the TAC) for both detectors was determined as 4 ns during the time calibration process since the best time resolution values were obtained at this delay time (Fig. 5).

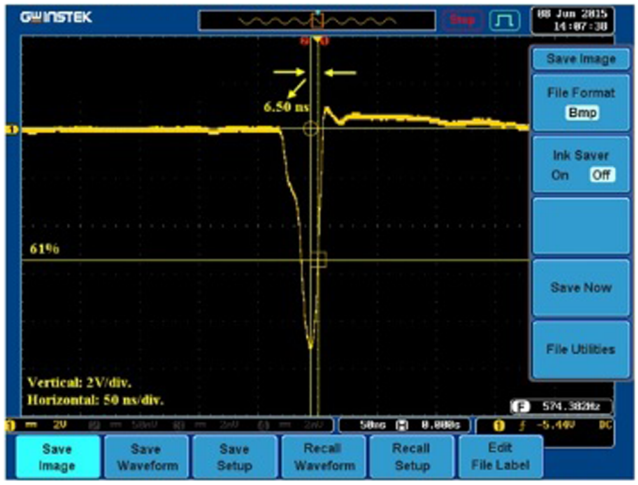
The detectors used in the spectrometers were simulated with FLUKA MC simulation program as described in the experiments above in order to support the experimental results with the theoretical method. In this program, scoring cards and physics lists are used to evaluate the required quantities. Further information about it can be found in the literature.[18,19] In our procedure, NaI(Tl) and plastic detectors with the same crystal thicknesses, and their positions were simulated as in the experiments. Figure 6 shows a sketch of the detectors and their positions obtained directly from the program. Additionally, 511 keV-energy photons were simultaneously sent to both crystals in the program. The distances between both detectors were fixed separately, and the detector counts were acquired through the program for each detector distance as in the experiments. PRECISIO physics list was used in these interactions. Finally, experimental and theoretical results were compared with each other for the sake of completeness.

Fig. 7 shows the TFA output signal shapes from the NaI(Tl) and the plastic scintillation detectors and calculated peaking and shaping time values obtained from an oscilloscope (GW Instek GDS-3504) with the sample rate of 4 GS/s. The peaking times and the shaping times for the NaI(Tl) and plastic scintillation detectors were determined to be 720 and 32 ns, 240 and 6.50 ns, respectively.

Reuse of AIP Publishing content is subject to the terms at: https://publishing.aip.org/authors/rights-and-permissions. Download to IP: 155.223.84.191 On: Mon, 17 Oct 2016 10:49:28

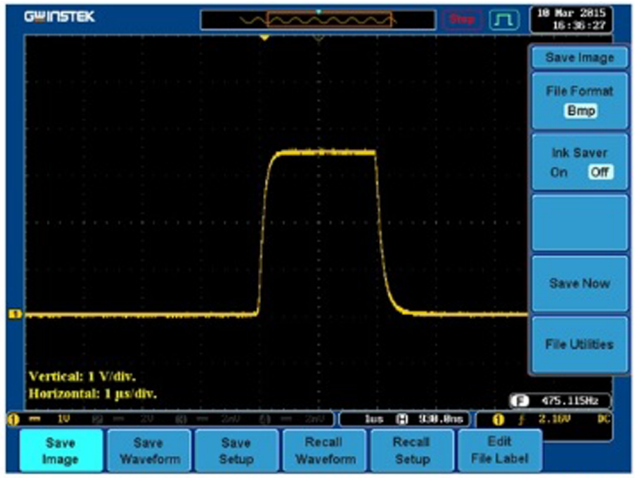


(a) Shaping time of the NaI(Tl) scintillation detector from the TFA.

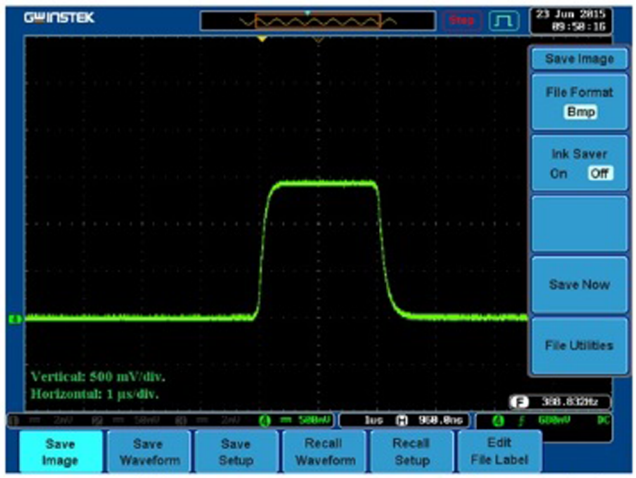


(b) Shaping time of the plastic scintillation detector from the TFA.

FIG. 7. (a) Shaping time of the NaI(Tl) scintillation detector from the TFA. (b) Shaping time of the plastic scintillation detector from the TFA.



(a) TAC output signal shape of the NaI(Tl) scintillation detector.



(b) TAC output signal shape of the plastic scintillation detector.

FIG. 8. (a) TAC output signal shape of the NaI(Tl) scintillation detector. (b) TAC output signal shape of the plastic scintillation detector.

In Fig. 8, the TAC output signal shapes of the detectors are given.

In the experimental section of the study, the distances of start and stop detectors from the source were set to 1 cm. This distance was called the reference point (d = 0 cm) which means that the distance was assumed to zero. The stop detector was fixed while the start detector was moved to distances of d = 2,4,6, and 8 cm from the source position. Time spectra were collected for each distance (d). As the start detector was placed in the distances of d = 2,4,6, and 8 cm, respectively, the channel numbers corresponding to the timing peak positions moved to higher channel numbers. This movement showed that a time delay occurred with respect to the reference point when the start detector was farther from the reference point. This change of the peak position (i.e., time delay or time difference) in the time spectrum was determined by subtracting the channel number of the peak position from the channel number corresponding to the reference point. These time differences were determined for each distance.

Since 1 m-cable length for RG-58 C/U coaxial cables generates a delay of 5 ns,[23] we calculated the cable lengths corresponding to these time differences for each distance. We then used these cables in different lengths in the start input of the

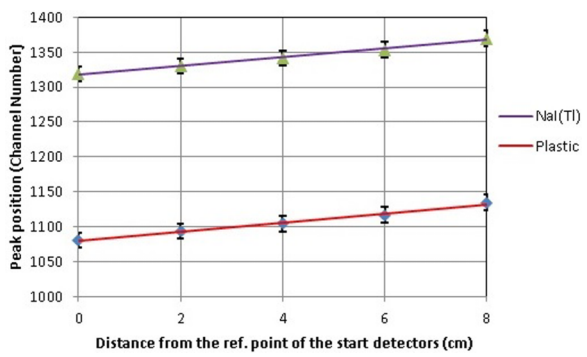


FIG. 9. Peak positions vs. distance from the reference point of the start detectors.

Reuse of AIP Publishing content is subject to the terms at: https://publishing.aip.org/authors/rights-and-permissions. Download to IP: 155.223.84.191 On: Mon, 17 Oct 2016 10:49:28

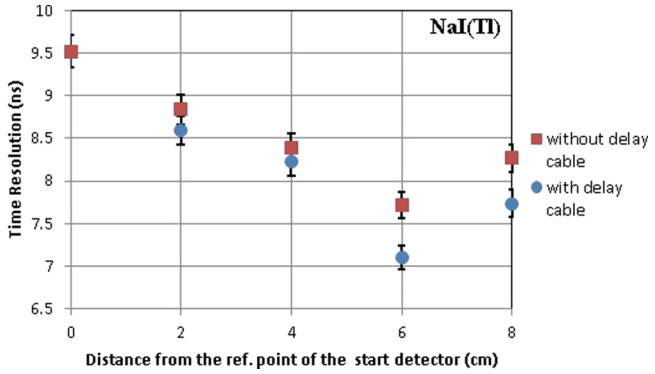


FIG. 10. Time resolution values with and without additional delay cables vs. distance from the reference point of the start detector for the NaI(Tl) scintillation detectors.

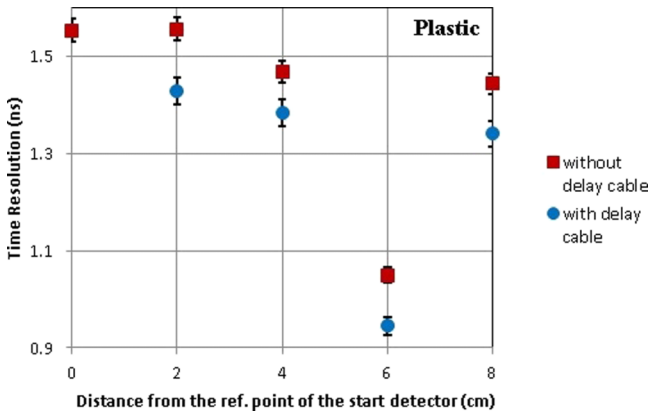


FIG. 11. Time resolution values with and without additional delay cables vs. distance from the reference point of the start detector for the plastic scintillation detectors.

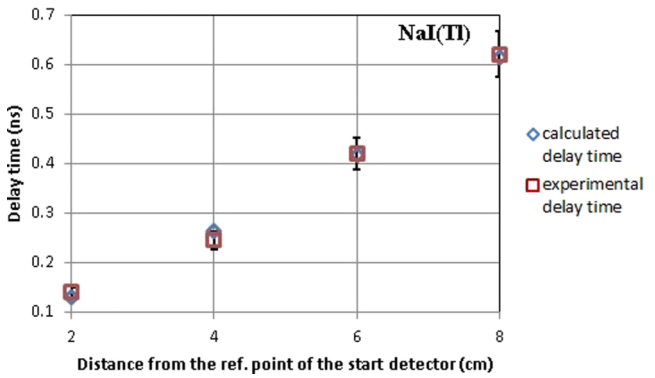


FIG. 12. Calculated and experimental delay times vs. distance from the reference point of the start detector for the NaI(Tl) scintillation detectors.

TAC separately. Thus, we compensated these time differences between start and stop inputs by this way. The time spectra for both spectrometers were acquired again and obtained results are given in Sec. III.

In the theoretical section of the study, the maximum counts corresponding to each distance from the reference point of the start detectors were determined. For this purpose, FLUKA MC program was used, and this simulation process was repeated for NaI(Tl) and plastic detectors. Comparison of the obtained experimental and theoretical results is given in Sec. III.

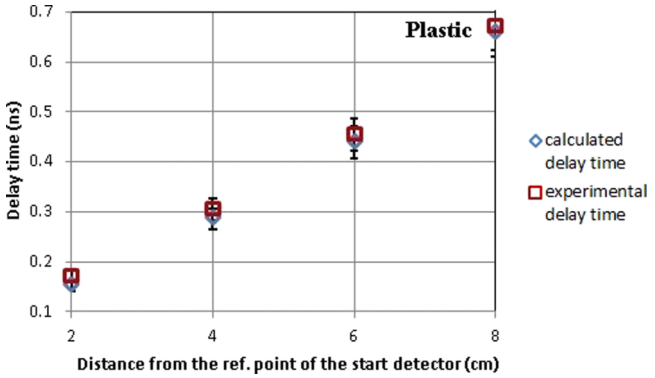


FIG. 13. Calculated and experimental delay times vs. distance from the reference point of the start detector for the plastic scintillation detectors.

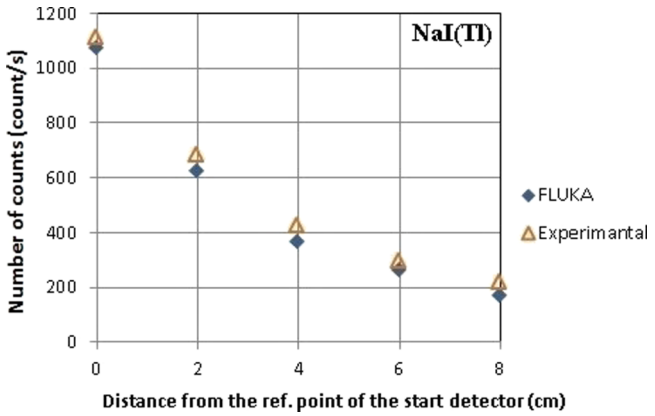


FIG. 14. Comparison of experimental and theoretical counts for the NaI(Tl) scintillation detectors with respect to the distance from the reference point of the start detector.

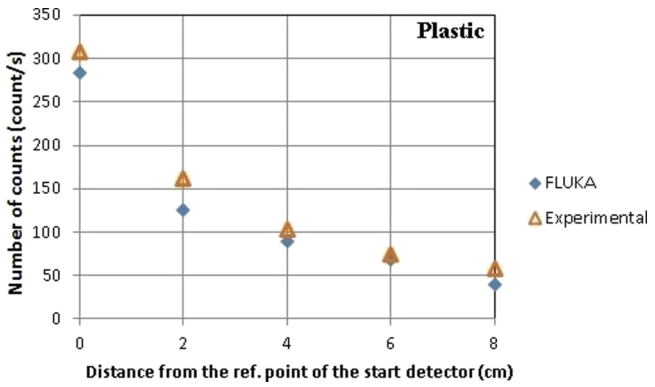


FIG. 15. Comparison of experimental and theoretical counts for the plastic scintillation detectors with respect to the distance from the reference point of the start detector.

III. RESULTS

Variations of the peak positions (channel number) versus distance from the reference point of the start detectors are given in Fig. 9.

In Figs. 10 and 11, obtained time resolution values with and without additional delay cables which were added the start input of the TAC are shown for both detectors, respectively. It can be deduced from the figures after a large number of tests that best time resolution would be able to acquire with the optimum detector position. As the start detector was moved

Reuse of AIP Publishing content is subject to the terms at: https://publishing.aip.org/authors/rights-and-permissions. Download to IP: 155.223.84.191 On: Mon, 17 Oct 2016 10:49:28

TABLE I. f values of the coincidence systems with and without additional delay cables.

	f value for whole-body (heavy)		f value for whole body (average)		f value for human brain	
Detectors	Without delay cable	With delay cable	Without delay cable	With delay cable	With delay cable	With delay cable
NaI(Tl)	0.30	0.33	0.23	0.25	0.17	0.19
Plastic	2.22	2.47	1.71	1.90	1.27	1.41

TABLE II. TOF gain values of the coincidence systems with and without additional delay cables.

	TOF gain (G) (for whole-body, heavy, D = 35 cm)		TOF gain (G) (for whole-body, average, D = 27 cm)		TOF gain (G) (for human brain, D = 20 cm)	
Detectors	Without additional delay cable	With additional delay cable	Without additional delay cable	With additional delay cable	Without additional delay cable	With additional delay cable
NaI(Tl)	0.55	0.57	0.48	0.50	0.42	0.43
Plastic	1.49	1.57	1.31	1.38	1.13	1.19

TABLE III. Experimental time resolution results of the coincidence systems with and without additional delay cables with respect to the distance from the reference point of the start detectors.

Distance from the reference point of the start detectors (d) (cm)	Time resolution (without additional delay cable) (ns)		Time resolution (with additional delay cable) (ns)	
	NaI(Tl)	Plastic	NaI(Tl)	Plastic
0.0	9.518 ± 0.324	1.553 ± 0.027	...	...
2.0	8.836 ± 0.336	1.555 ± 0.127	8.594 ± 0.341	1.428 ± 0.110
4.0	8.392 ± 0.345	1.467 ± 0.039	8.220 ± 0.349	1.384 ± 0.066
6.0	7.714 ± 0.360	1.050 ± 0.037	7.098 ± 0.375	0.945 ± 0.044
8.0	8.264 ± 0.347	1.443 ± 0.095	7.736 ± 0.360	1.340 ± 0.088

far away from the reference point, moreover, the "start" signal of the TAC delayed and thus, the time difference between start and stop detectors decreased, leading to resolution enhancement. As a principle, "start" input of TAC should be furnished first with respect to the "stop" input for generating a logic output. Since "start" input have gradually delayed than that of the "stop" one at the distances farther than 6 cm, the resolution has normally started to deteriorate.

Experimental and calculated delay times (time differences) which were mentioned in Sec. II are compared for both detectors in Figs. 12 and 13.

FLUKA program generated the coincidence counts for start and stop detectors as a function of the distance between them. In order to support the experimental counts, these theoretical counts are compared with them for both detector types in Figs. 14 and 15, respectively.

Spatial resolution values (Δx) were calculated for the coincidence system of plastic detectors with and without additional delay cables due to its fast response. The equation given in the "Introduction" section was used for this calculation, and these values were found as 15.75 and 14.18 cm, respectively. Hence, an improvement in the spatial resolution of almost 9.9% was determined for the whole-body imaging.

D value in the f relation depends on the body volume. In this respect, the f values calculated for the human whole-body (heavy, D = 35 cm; average D = 27 cm) and brain (D = 20 cm) are indicated in Table I. Since the D value is 20 cm for a thin human whole-body like in brain,[12] its calculated f value has not been given in the results here in order to prevent the duplication. The positive effect of the additional delay can clearly be observed in the table.

TOF gain (G) values for the whole body (heavy and average) and brain are also given in Table II.

From this table, it can be said that the additional delay to the start signal has contributed to the TOF gain (SNR gain) or time resolution (coincident resolving time) enhancement.

In Table III, calculated time resolution values for both spectrometers with and without additional delay cables at different distances from the reference point of the start detector are tabulated.

As stated previously, the delay times were determined using the peak positions corresponding to each distance in the time spectra. These peak positions were subtracted from the positions of the reference points for the detectors. Therefore, time resolution values of both detectors for reference point in the first right cells in Table III are blank.

IV. CONCLUSIONS AND DISCUSSION

Several studies have shown that the time resolution value for the coincidence measurements in medical imaging systems

Reuse of AIP Publishing content is subject to the terms at: https://publishing.aip.org/authors/rights-and-permissions. Download to IP: 155.223.84.191 On: Mon, 17 Oct 2016 10:49:28

was a crucial parameter since it was effective on the measurements' quality.[3,6,8,10,11,14,15]

The constant fraction timing method and the start-stop coincidence timing spectrometer composed of organic (BC412) and inorganic (NaI(Tl)) scintillation detectors were used here like in our previous study[20] in order to show the reliability of the obtained results and to support the results and conclusions given there.

Generally, the results obtained using the plastic detectors were better than the results obtained using the NaI(Tl) scintillation detectors due to faster decay times of plastic scintillators. Therefore, used BC412 type plastic detectors were suitable for TOF/PET coincidence systems.

If time resolution, SNR gain, and spatial resolution of a coincidence system are favorable, the quality of medical imaging will be highly satisfactory in a PET system. So, in the present work, to enhance the time resolution of a coincidence spectrometer, the fast signal from the start detector at different distances from the reference point was delayed before the timing process. This delay has improved the spectrometers' time resolution, as shown in Table III. Thus, validity of our suggested method in our previous work has been proven once more by the presented study in enhancing the coincidence time resolution of a timing coincidence spectrometer using the additional delay cables (Tables I–III). The authors believe that this situation will help to improve the medical image quality on the basis of obtained results.

The distance between reference point and start detector was increased to 2, 4, 6, and 8 cm for each detector type. When the distance between source and the start detector was 6 cm, the best time resolution values with and without additional delay cables were achieved for both detector types (Figs. 10 and 11, Table III). This situation pointed out that there might be an optimum distance between the detectors with respect to the source position for the best timing detection performance.

Obtained calculated and experimental delay times for NaI(Tl) and plastic detectors were compared in Figs. 12 and 13. As it can be seen from the figures, these delay times were quite close to each other for each distance. This result showed us that the obtained experimental results with the additional cable length were reliable. Additionally, it has been noticed that the FLUKA results were compatible with the experimental timing ones though they were the coincidence counts obtained from the computation. These comparisons are given in Figs. 14 and 15.

Enhancement in f values, time and spatial resolutions and SNR gain obtained here for both detector types have consolidated the validity of the method proposed in our previous and present works.

This work demonstrated that the proposed method in our previous work and here succeeded in enhancing the time resolution of a start-stop coincidence system, spatial resolution, G and f values for human whole-body (heavy, average and thin) and brain imaging using a TOF/PET spectrometer.

As stated in the equations in the first section, spatial resolution and TOF gain depend on the time resolution of the coincidence system.[3,4,7,12,15,16,28–35] In other words, as the time resolution is enhanced, these parameters have more favorable values. Since the better TOF gain (i.e., SNR gain) means the better localization of the coincident events, this result will generate more significant improvement on the true coincident event, leading to better image quality. This important conclusion will be extremely effective on large or heavy patient bodies (Tables I and II).

Consequently, better resolutions will help the improvement not only on the TOF gain but also on the spatial resolution. This will lead to better images and can help the Physician in his/her diagnosis and treatment. In addition, time saving, lower cost, patient comfort, and pleasure can be provided as the other benefits of the resolution enhancement in the long run.[8]

ACKNOWLEDGMENTS

This work was supported by TUBITAK, the Scientific and Technological Research Council of TURKEY under Project No. 197T087, by EBILTEM, Center of Science and Technology, Ege University under Project No. 99 BIL 001, by Research Fund of Uludag University under Project No. OUAP(F)-2012/26, and by Research Fund of Ege University under Project No. 14 FEN 026.

[1]J. J. P. De Lima, *Nuclear Medicine Physics* (Taylor & Francis, USA, 2011).
[2]G. F. Knoll, *Radiation Detection and Measurements* (John Wiley & Sons Inc., New York, 2000).
[3]M. Ahmed, B. Camanzi, and J. Matheson, Nucl. Instrum. Methods Phys. Res., Sect. A **695**, 252 (2012).
[4]W. S. Choong, Phys. Med. Biol. **54**, 6495 (2009).
[5]D. L. Snyder, L. J. Thomas, and M. M. Ter-Pogossian, IEEE Trans. Nucl. Sci. **28**, 3575 (1981).
[6]W. W. Moses, IEEE Trans. Nucl. Sci. **50**, 1325 (2003).
[7]K. Shibuya, H. Saito, M. Koshimizu, and K. Asai, Appl. Phys. Express **3**, 086401 (2010).
[8]M. Conti, Phys. Med. **25**, 1 (2009).
[9]M. E. Casey, http://scipp.ucsc.edu/~hartmut/UFSD/Simens_ultraHD-PET_White_Paper.pdf, accessed 15 April 2016.
[10]T. Budinger, J. Nucl. Med. **24**, 73 (1983).
[11]M. Conti, B. Bendriem, M. Casey, M. Chen, F. Kehren, C. Michel, and V. Panin, Phys. Med. Biol. **50**, 4507 (2005).
[12]J. S. Karp, S. Surti, M. E. Daube-Witherspoon, and G. Muehllehner, J. Nucl. Med. **49**, 462 (2008).
[13]L. Friscic, D. Bosnar, M. Distler, and M. Makek, https://indico.cern.ch/event/51276/contribution/237/material/paper/1.pdf, accessed 15 April 2016.
[14]W. W. Moses, Nucl. Instrum. Methods Phys. Res., Sect. A **580**, 919 (2007).
[15]M. Conti, IEEE Trans. Nucl. Sci. **53**, 1188 (2006).
[16]R. L. Harrison, A. M. Alessio, P. E. Kinahan, and T. K. Lewellen, in *IEEE Nuclear Science Symposium Conference Record* (IEEE, 2004), p. 4080.
[17]S. P. Bönisch, *Electronics for Radiation Detection* (CRC Press, USA, 2011).
[18]A. Ferrari, P. R. Sala, A. Fasso, and J. Ranft, CERN, INFN/TC_05/11, SLAC-R-773, 2005.
[19]G. Battistoni, F. Cerutti, A. Fasso, A. Ferrari, S. Muraro, J. Ranft, S. Roesler, and P. R. Sala, AIP Conf. Proc. **86**, 31 (2007).
[20]E. E. Ermis, C. Celiktas, and E. Pilicer, Radiat. Meas. **62**, 52 (2014).
[21]Rexon Components, Inc., NaI(Tl) Scintillation Crystal Specifications, http://www.rexon.com/NaITlBlanksSpecs.pdf, accessed 15 April 2016.
[22]Saint-Gobain plastic Scintillator, http://www.crystals.saint-gobain.com/uploadedFiles/SG-Crystals/Documents/Physcial%20Constants%20chart.pdf, accessed 15 April 2016.
[23]R. W. Leo, *Techniques for Nuclear and Particle Physics Experiments* (Springer–Verlag, Germany, 1994).
[24]N. Tsoulfanidis, *Measurements and Detection Radiation* (Taylor & Francis, USA, 1995).
[25]P. W. Nicholson, *Nuclear Electronics* (John Wiley & Sons Inc., New York, 1974).
[26]M. O. Bedwell and T. J. Paulus, IEEE Trans. Nucl. Sci. **23**, 234 (1976).

Reuse of AIP Publishing content is subject to the terms at: https://publishing.aip.org/authors/rights-and-permissions. Download to IP: 155.223.84.191 On: Mon, 17 Oct 2016 10:49:28

[27]J. Vacik, J. Cervena, V. Hnatowicz, H. Havranek, J. Hoffmann, S. Posta, D. Fink, and R. Klett, Nucl. Instrum. Methods Phys. Res., Sect. B **142**, 397 (1998).
[28]M. Conti, Nucl. Instrum. Methods Phys. Res., Sect. A **648**, S194 (2011).
[29]S. Krishnamoorthy, B. Legeyt, M. E. Werner, M. Kaul, F. M. Newcomer, J. S. Karp, and S. Surti, IEEE Trans. Nucl. Sci. **61**, 1092 (2014).
[30]S. Krishnamoorthy, R. I. Wiener, M. Kaul, J. Panetta, J. S. Karp, and S. Surti, *IEEE Nuclear Science Symposium Conference Record* (IEEE, 2011), p. 2457.
[31]S. Surti, J. S. Karp, L. M. Popescu, M. E. Daube-Witherspoon, and M. Werner, IEEE Trans. Med. Imaging **25**, 529 (2006).
[32]M. Conti, Eur. J. Nucl. Med. Mol. Imaging **38**, 1147 (2011).
[33]J. Torres, R. Garcia, A. Aguilar, J. Soret, J. Martos, A. J. Gonzalez, F. Sanchez, J. M. Benlloch, and M. J. Rodriguez, in *Implementation of TOF-PET Systems on Advanced Reconfigurable Logic Devices*, edited by S. Misciagna (InTech, 2013).
[34]S. Surti, J. Nucl. Med. **56**, 98 (2015).
[35]S. Surti and J. S. Karp, Phys. Med. **32**, 12 (2016).

Reuse of AIP Publishing content is subject to the terms at: https://publishing.aip.org/authors/rights-and-permissions. Download to IP: 155.223.84.191 On: Mon, 17 Oct 2016 10:49:28